Research Repository UCD

Provided by the author(s) and University College Dublin Library in accordance with publisher policies. Please cite the published version when available.

Title	Nanoparticle Adhesion to the Cell Membrane and Its effect on Nanoparticle Uptake Efficiency
Author(s)	Lesniak, Anna; Salvati, Anna; Santos-Martinez, Maria J.; Radomski, Marek W.; Dawson, Kenneth A.; Åberg, Christoffer
Publication date	2013-01-09
Publication information	Journal of the American Chemical Society, 135 (4): 1438-1444
Publisher	American Chemical Society
Item record/more information	http://hdl.handle.net/10197/4575
Publisher's statement	This document is the Accepted Manuscript version of a Published Work that appeared in final form in Journal of the American Chemical society, copyright © American Chemical Society after peer review and technical editing by the publisher. To access the final edited and published work see http://pubs.acs.org/doi/abs/10.1021/ja309812z.
Publisher's version (DOI)	http://dx.doi.org/10.1021/ja309812z

Downloaded 2018-04-23T19:46:46Z

The UCD community has made this article openly available. Please share how this access benefits you. Your story matters! (@ucd_oa)

Some rights reserved. For more information, please see the item record link above.

Nanoparticle adhesion to the cell membrane and its effect on nanoparticle uptake efficiency

Anna Lesniak,[1,†] *Anna Salvati,*[1,†] *Maria J. Santos-Martinez,*[2,3,4] *Marek W. Radomski,*[2,4] *Kenneth A. Dawson,*[1,*] *Christoffer Åberg*[1,*]

[1] Centre for BioNano Interactions, School of Chemistry and Chemical Biology, University College Dublin, Belfield, Dublin 4, Ireland

[2] The School of Pharmacy and Pharmaceutical Sciences, Trinity College Dublin, Dublin 2, Ireland.

[3] School of Medicine, Trinity College Dublin, Dublin 2, Ireland.

[4] Trinity Biomedical Sciences Institute, Trinity College Dublin, Dublin 2, Ireland.

KEYWORDS nanomaterials, adsorption, lipid bilayer, quartz crystal microbalance, protein corona, serum free

ABSTRACT: The interactions between nano-sized particles and living systems are commonly mediated by what adsorbs to the nanoparticle in the biological environment, its 'biomolecular corona', rather than the pristine surface. Here we characterise the adhesion towards the cell membrane of nanoparticles of different material and size, and study how this is modulated by the presence or absence of a corona on the nanoparticle surface. The results are corroborated with adsorption to simple model supported lipid bilayers using a quartz crystal microbalance. We conclude that the adsorption of proteins on the nanoparticle surface strongly reduces nanoparticle adhesion in comparison to what is observed for the bare material. Nanoparticle uptake is described as a two-step process, where the nanoparticles initially adhere to the cell membrane and subsequently are internalised by the cells via energy-dependent pathways. The lowered adhesion in the presence of proteins thereby causes a concomitant decrease in nanoparticle uptake efficiency. The presence of a biomolecular corona may confer specific interactions between the nanoparticle-corona complex and the cell surface, including triggering of regulated cell uptake. An important effect of the corona is, however, a reduction in the purely unspecific interactions between the bare material and the cell membrane, which in itself disregarding specific interactions, causes a decrease in cellular uptake. We suggest that future nanoparticle-cell studies include, together with characterisation of size, charge and dispersion stability, an evaluation of the adhesion properties of the material to relevant membranes.

Introduction

There is currently growing interest in how nanoparticles (NPs) interact with living systems, both from the point of view of the safe implementation of nanotechnology,[1-7] as well as from an improved drug delivery perspective.[8,9] Previous studies have shown that the uptake of NPs by living cells is affected by NP properties such as size[10-13] and surface.[14-16] However, NPs dispersed in a biological fluid are rapidly covered by biomolecules, such as proteins and lipids, forming a biomolecular 'corona' that effectively screens the bare NP surface.[17-22] When cells are exposed to NPs it is therefore, in realistic circumstances, typically not the bare NP surface that interacts with the cell but the NP-biomolecular corona complex.[23-25] Consequently, it becomes interesting to correlate NP uptake not to properties of the bare NP, but to properties of the NP-biomolecular corona complex.[26,27]

NP uptake begins with an initial adhesion of the NP to the cell and interactions with the lipids, proteins and other components of the cell membrane. This is followed by the activation of an energy-dependent uptake mechanism,[10,11,14] which allows the NPs to be internalised into the cell and further trafficked to different subcellular locations, typically ending in lysosomal accumulation.[10,28,29] One of the key steps in NP uptake efficiency is therefore the starting NP adhesion to the cell membrane. Previous studies have investigated this aspect, for example by exposing cells to NPs at 4 °C to inhibit internalisation[30-32], or by dissolving NPs on the outside of the membrane.[15] Information on NP adhesion to membranes composed solely of lipids is also emerging by studying their adsorption onto micron-sized particles coated with lipids.[33]

In this work we have investigated the adhesion properties of NPs with a particular emphasis on the effect of the biomolecular corona. Interactions between biomolecules in the corona and corresponding receptors in the cell membrane may trigger biological recognition and uptake of the NP-corona complex. It has, furthermore, been shown that corona biomolecules can interact with membrane receptors to induce cell-signaling response.[34] In both cases, the response is due to a specific interaction between corona biomolecules and components of the cell membrane. However, it is important not to disregard unspecific interactions and the adhesion properties they lead to. Thus NPs with high energy of the bare surface typically adsorb strongly to cell membranes because of unspecific interactions, thereby lowering their surface energy. In the presence of biomolecules, however, the formation of a NP corona has already lowered the surface energy and unspecific interactions between the NP-corona complex and the cell membrane are much reduced. For example, while 50 nm silica nanoparticles cause strong damage to cells when exposed in the absence of serum, the damage is mitigated in the presence of serum, an effect that can be related to the adhesion properties of the nanoparticles in the two conditions.[35]

Here we study the detailed kinetics and concentration-dependence of the adsorption process of nanoparticles of different size and material. We show that the presence or absence of serum in the NP dispersion strongly affects the adhesion properties of NPs to the cell membrane, and that this accounts, at least partially, for a corresponding difference in NP-uptake levels. We furthermore corroborate our findings by studying NP-adsorption onto supported lipid bilayers by quartz crystal microbalance. From a broader perspective, the results reinforce the prime importance of the biological milieu in NP-cell interactions.

Results and Discussion

Human adenocarcinomic alveolar basal epithelial A549 cells were used as model cells in this study. They were exposed to carboxylated polystyrene NPs (PS-COOH) of diameter 40 and 100 nm, as well as unmodified silica NPs (SiO_2) of diameter 50 nm. Particle characterisation in relevant media is shown in Supplementary Table S1. All NPs are fluorescently labelled which allows the measurement of the fluorescence of NPs associated with cells, i.e. adhering to the outer membrane or internalized, on a per cell basis by flow cytometry. All experiments were performed in at least two types of medium: serum free medium (sfMEM) and complete cell culture medium supplemented with 10% foetal bovine serum (cMEM). A range of nanoparticle concentrations were used. We note that varying NP concentration, and hence the total NP surface area available, but keeping the serum concentration constant, implies that the ratio of protein content to NP surface area varies.

Kinetics of nanoparticle uptake

An example of NP uptake by cells is shown in Figure 1, where A549 cells have been continuously exposed to 40 nm PS-COOH for the indicated times. The reported values are the mean cell fluorescence due to the NPs per cell. Clearly NP uptake is higher under serum free conditions (sfMEM) compared to what is observed in the presence of proteins (cMEM), as reported for silica nanoparticles in our previous work,[35] as well as for several other systems in the literature.[36-39] This can be related to the absence of proteins on the NP surface in the starting dispersion, prior to addition to cells. However, it should be noted that even under serum-free conditions some proteins can be found on the NPs after incubation with cells for some time, probably originating from cell secretions and cell damage[35].

Part of the proteins, the so-called 'hard corona' associated with the NPs are so strongly bound to the NPs that NP-protein complexes can be isolated from a NP dispersion[19] and re-suspended in serum free medium. In this way it is possible to demonstrate the effect of the hard corona protein layer on NP uptake and exclude other effects due to the presence of serum in the medium, such as crowding and/or competition for the cell membrane and membrane receptors by the serum proteins. Figure 1 shows the uptake also of such hard corona-covered NPs re-suspended in serum free medium (HC+sfMEM). Their uptake is much lower than for NPs added to cells in the absence of proteins (sfMEM), thus confirming that protein adsorption to NPs reduces NP uptake.

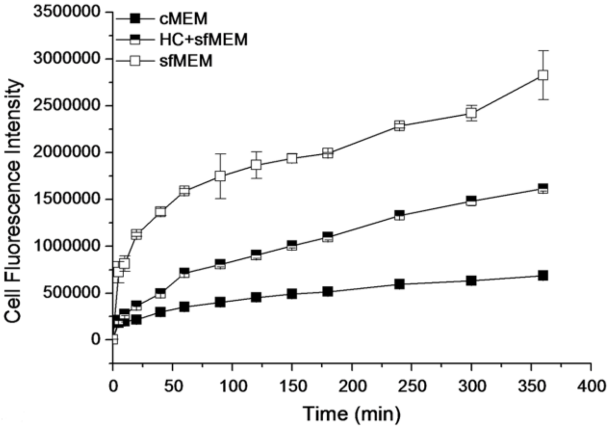

Figure 1. Kinetics of uptake of 100 μg/ml fluorescently labelled 40 nm PS-COOH NPs by A549 cells during continuous exposure, as determined by flow cytometry. Cells were exposed to NPs in complete medium (cMEM), NPs in serum free medium (sfMEM) and hard corona-NP complexes in serum free medium (HC+sfMEM). The mean cell fluorescence of 15,000 cells was determined for each replica. Data points and error bars represent the mean and standard deviation over three replicas. The curve in complete medium is shown alone in Supplementary Figure S1.

Under all three conditions, the uptake kinetics exhibits a similar behaviour with an initial transient followed by an essentially linear uptake. We argue that this behaviour originates from the two processes of (i) NPs adhering to the outer cell membrane and (ii) actual internalisation.[30] During the initial transient, NPs reach and adhere to the cells, but internalisation is slower. After some time, a steady state is reached, where the number of NPs reaching and adhering to cells is balanced by internalisation, consistent with linear uptake. At even longer times cell division will dilute the NP load,[28,29,40] but this is a negligible process at these short times. This view suggests that a principal determinant of NP uptake by cells is the adhesion properties of the NP to the outer cell membrane.

Nanoparticle adhesion to cells

The adhesion properties of a NP to the cell membrane are, however, difficult to disentangle in the presence of simultaneous internalisation, such as in the experiments shown in Figure

1. Since several active processes, including NP uptake,[28,29] are shut down at 4 °C, previous work has measured NP adhesion to the cell membrane by incubating cells with NPs at 4 °C.[30,31] Indeed, after incubation at 4 °C, 40 nm PS-COOH NPs can be seen adhered to the cell membrane by confocal microscopy (Supplementary Figure S2). However, after removal of the medium containing NPs and further incubation in NP-free medium at 4 °C, we observed a decrease in the cell fluorescence signal with time (Supplementary Figure S2) suggesting partial desorption of the NPs from the cell membrane. The decrease of fluorescence with time makes the experiments somewhat practically cumbersome. Moreover, we found that it was difficult to reproduce and quantify the cell fluorescence when measured directly after NP adhesion at 4 °C (see Supplementary Figure S2 for details). We therefore chose to follow the incubation with NP-containing medium at 4 °C with further incubation in NP-free medium at 37 °C, allowing active processes to be restored and the adhering NPs to enter the cells. Using this procedure, cell fluorescence remained fairly constant with time (Supplementary Fig. S2), aiding quantification. Cells were also observed with confocal microscopy during the incubation at 37 °C, in order to ensure proper restoration of active processes following the 4 °C pre-incubation. We did not observe any abnormal features of the cells, and the 40 nm PS-COOH NPs to a large extent follow the endo-lysosomal pathway (Supplementary Figure S3), as they do in the absence of the 4 °C pre-incubation.[26,28]

As it may be of a somewhat general nature for fluorescently labeled NPs, we mention one further technical detail: Even though the fluorescent label is in the NP core, there is still a small release of the label from the NPs once they are inside cells[28,41]. However, once the NP source is removed, the free fluorescent label exits cells within minutes[28] (Supplementary Figure S2). A further advantage in following the NP exposure at 4 °C with a 3 h incubation in NP-free medium at 37 °C is therefore that the little free dye that is present has plenty of time to exit the cells prior to assessment.

In summary, we ultimately chose to measure NP adhesion to the cell membrane by following the exposure to NPs at 4 °C with a 3 h incubation in NP-free medium at 37 °C prior to assessment by flow cytometry. The procedure, illustrated schematically in Figure 2a-b, allowed a reproducible quantification of the adhesion of the NPs to the cell membrane. In this way, we can study the progressive adhesion of the NPs to the cell membrane with increasing exposure to NPs at 4 °C.

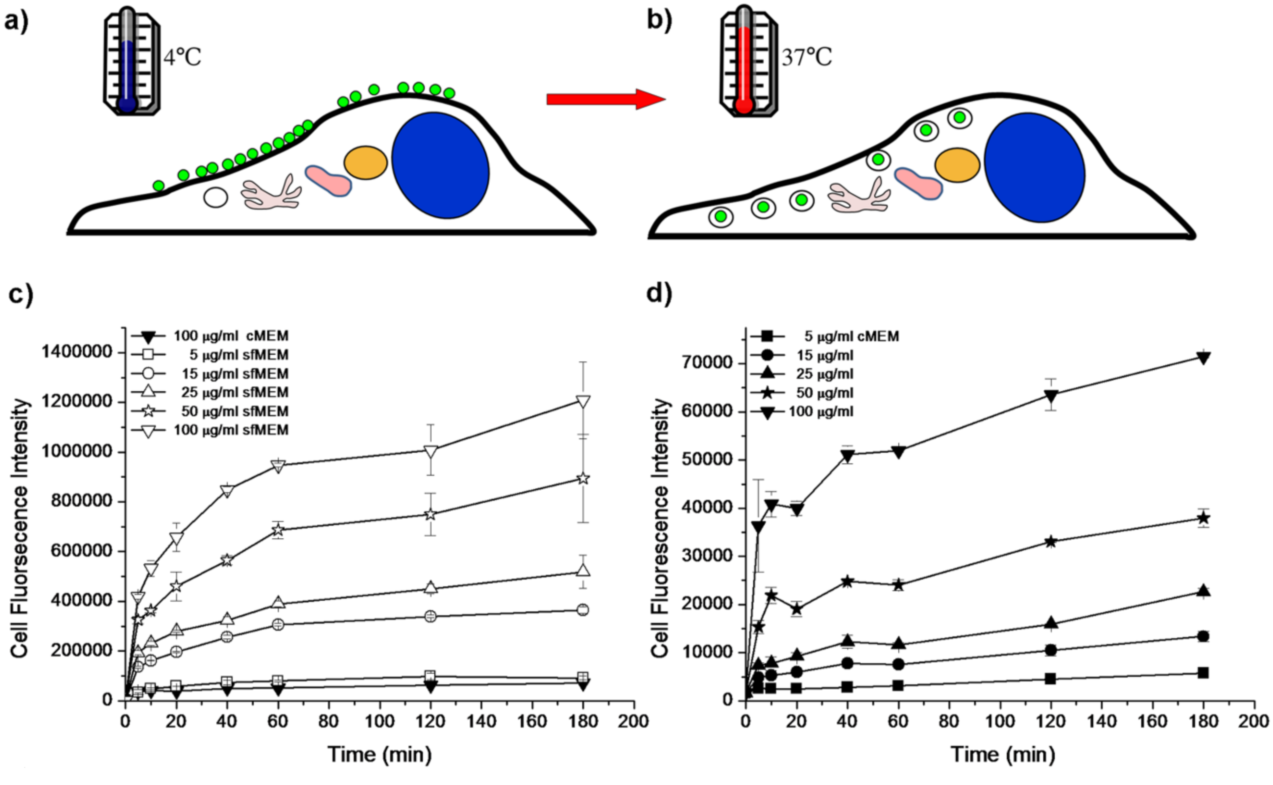

Figure 2. Adhesion of 40 nm PS-COOH NPs onto the cell membrane of A549 cells, measured by flow cytometry. (a-b) Schematic illustrating the procedure to measure NP adhesion to the cell membrane. (a) Cells were exposed to NP-containing medium at 4 °C. At 4 °C NP uptake is suppressed and the NPs simply adhere to the outer cell membrane. (**b**) After few washes, the NP dispersion is replaced by NP-free medium and cells further incubated at 37 °C. At 37 °C the NPs adhering to the outer cell membrane are internalised, and the NPs originally adhering to the cell membrane, which are now inside the cells, can be quantified. (c-d) Experimental data showing the adsorbed amount as a function of time under serum free conditions (c) and in complete medium (d). In panel c the adsorption obtained when exposing cells to the highest NP concentration in complete medium is also included as a reference. Data points and error bars represent the mean and standard deviation over three replicas. The adsorbed amount as a function of concentration is reported in Supplementary Figure S7.

Figure 2c-d shows the adhesion, obtained as just described, of 40 nm PS-COOH to the cell membrane of A549 cells as a function of time and for a range of different NP concentrations. As expected by the uptake levels shown in Figure 1, NPs under serum free conditions (Figure 2c) exhibit a much higher adhesion to the cell membrane compared to when the NP surface is covered by proteins (Figure 2d). This observation holds true for all concentrations, and is corroborated for 100 nm PS-COOH and 50 nm SiO_2, as shown in Supplementary Figures S4-5.

In complete medium (Figure 2d), the kinetics exhibits signs of two processes: during the first 10 min the adsorbed amount increases rapidly, while after that the adsorption grows much slower. A similar observation can be made in serum free medium (Figure 2c), though it is somewhat less clear. Previous studies[30] have described the adsorption process following Langmuir, *viz*

$$dN_m/dt = k_{0m}c_0(N_{m,max} - N_m) - k_{m0}N_m \qquad (1)$$

where $N_m(t)$ is the number of NPs adsorbed to the membrane at time t, c_0 is the concentration of NPs in the extracellular medium, $N_{m,max}$ is the maximum possible number of NPs adsorbed to the membrane and k_{0m} and k_{m0} are rate constants for the adsorption onto and desorption from the membrane, respectively. However, as the data in Figure 2 exhibit two kinetic processes, it is impossible to obtain a good fit with this approach.

As to the origin of two processes, there are several candidates. One possibility under complete medium conditions (Figure 2d), especially considering that the NPs and the serum-containing medium are mixed just before exposure to cells, is that one process represents NPs incompletely covered by protein and the other fully-covered NPs. However, two processes can also be seen in the absence of serum (Figure 2c). Furthermore when NPs were incubated for 1 h in complete medium prior to addition to cells, the kinetics still exhibits sign of multiple processes (Supplementary Figure S6). A different possibility is the creation of new available surface for the NPs to adsorb to. In principle, there is new membrane surface created during cell growth, but since the full cell cycle is 22 h for A549 cells[40], the rate of cell cycle progression is too low to justify the full observed increase. A third possibility is binding to two different types of receptors of different affinity, but the similar kinetics under serum-free and complete medium conditions speaks against that. A fourth possibility is that the NPs adsorb in several layers on the cells. This might be particularly relevant under serum free conditions, where electron microscopy of cells exposed to silica NPs suggested adsorption of the NPs to the cells in several 'loosely defined' layers.[35] A final possibility is that the initial fast increase is from the hydrodynamic flow created when the NP dispersion is added to the cell culture. At the moment, we cannot differentiate further between these different possibilities.

Though the damage to the cells if kept for longer times at 4 °C prevents us from reaching full equilibrium, the results in Figure 2c-d also suggest that the adsorbed amount at equilibrium is concentration-dependent, under both serum free and complete medium conditions. This is consistent with NPs being able to desorb from the cell membrane, as was observed when cells were kept at 4 °C after removal of the NP-containing medium (Supplementary Figure S2).

Supplementary Figure S7 shows the same data as in Figures 2c-d, but plotted as a function of concentration for fixed times. Under serum free conditions, the adsorbed amount shows a tendency to saturate with increasing concentration, though for the highest concentration investigated here, the limit is not yet reached. In the presence of serum there is no sign of saturation, consistent with adsorption being vastly lower compared to under serum-free conditions.

Nanoparticle adhesion to lipid bilayers

Comparative studies were performed on supported model lipid bilayers on silica surfaces, using a Quartz Crystal Microbalance with Dissipation monitoring (QCM-D). Bilayers composed of 2-Oleoyl-1-palmitoyl-*sn*-glycero-3-phosphocholine (POPC) were formed by surface-mediated vesicle fusion (Supplementary Figure S8).[42,43] Using QCM-D one can monitor the kinetics of adsorption of small molecules, proteins or, in our case, NPs onto the lipid film. A relevant example is when the POPC bilayer is formed under serum free conditions and complete medium with protein (cMEM) is subsequently perfused into the system (Supplementary Figure S8). Protein adsorb rapidly to the bilayer, forming an adsorbed layer that is stable for long perfusion times. Since the proteins adsorbed to the bilayer may shield the interactions with the nanoparticles, we used hard corona-covered NPs re-suspended in serum free medium, rather than NPs suspended in complete medium, in the bilayer adsorption studies.

Since the frequency shift measured by QCM-D is related to the adsorbed mass, we mainly acquired data for the SiO_2 NPs, which are heavier (density ~2.0 g/cm^3) than the polystyrene NPs (density ~1.05 g/cm^3). Figure 3a shows the adsorption of 50 nm SiO_2 NPs to the POPC bilayer. For bare NPs we observe a strong adsorption for all concentrations. In contrast, for hard corona-covered NPs little to no adsorption occurs even for the highest NP concentration. The same behavior was observed for 100 nm PS-COOH and 200 nm SiO_2, as shown in Figure 3c-d. These results corroborate the conclusions from the cell studies (Figure 2 and Supplementary Figure S4-5), where NPs in serum free conditions also showed a much higher adsorption to the cell membrane compared to protein-covered NPs. The same conclusions can be drawn for NPs in complete medium (Supplementary Figure S9).

Figure 3a also shows that the equilibrium adsorption is independent of the concentration of the 50 nm SiO_2 NPs, though the kinetics clearly is concentration dependent. As the frequency change due to adsorption of 200 nm SiO_2 NPs under serum free conditions (Figure 3d) is much higher than that of the 50 nm SiO_2 NPs (Figure 3a), we argue that the equilibrium signal is not due to having reached the limit of detection of the instrument. An equilibrium adsorption independent of concentration suggests that there is no desorption of the NPs from the lipid bilayer. Indeed, if the 50 nm SiO_2 NPs are let adhere to the POPC bilayer and NP-free serum free medium is perfused into the system, no significant change in adsorption can be seen (Figure 3b), showing the negligible desorption.

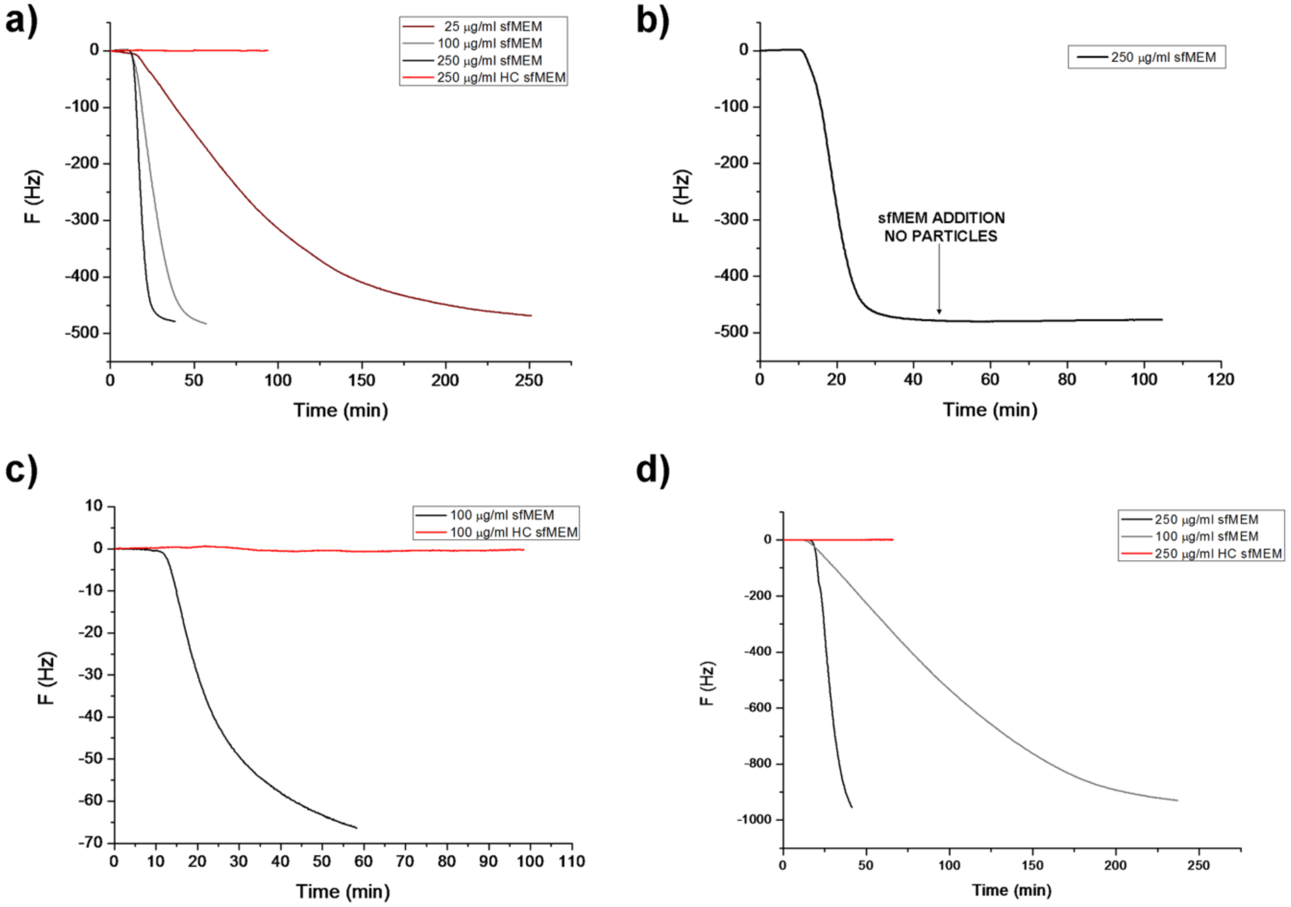

Figure 3. Adsorption of NPs with and without a hard corona onto supported POPC lipid bilayers on silica coated quartz crystal sensors obtained by QCM-D. Results are shown in terms of the shift in frequency of the third overtone. Time is measured from the moment of NP injection into the perfusion system; the actual arrival of the NPs to the sensor occurs some 15 min later. (a) Bare 50 nm SiO_2 NPs at different concentrations (sfMEM), and at the highest concentration for hard corona-covered NPs (HC sfMEM), all suspended in serum free medium. (b) Adsorption of 50 nm SiO_2 NPs at 250 μg/ml under serum-free conditions, and subsequent perfusion of NP-free serum free medium starting from the indicated time. The insignificant change in frequency after removal of the NP-containing medium shows that desorption of the NPs is negligible. (c) Adsorption of bare (sfMEM) and hard-corona covered (HC sfMEM) 100 nm PS-COOH suspended in serum free medium. (d) Adsorption of bare and hard-corona covered 200 nm SiO_2 in serum free conditions. NPs exposed in the presence of complete medium show similar results as the hard-corona covered NPs (Supplementary Fig. S9).

Nanoparticle adhesion and uptake

Having characterised NP adhesion to cells and simple lipid membranes, we are now in a position to discuss the importance of the adhesion step to NP uptake. Figure 4a compares the kinetics of 40 nm PS-COOH uptake during continuous exposure (similar to Figure 1) with the kinetics of NP adhesion (similar to Figure 2). It is clear that, after some time, the number of NPs adhering to the outer cell membrane is low compared to the number of NPs inside cells. Nevertheless, the adhesion process is likely still of prime importance.

To illustrate this point, we consider the uptake rate of 40 nm PS-COOH in complete medium as a function of NP concentration, which is reproduced from our previous work[28] in Figure 4b. For simplicity taking into account only one adsorption process, we can extend Equation (1) to include NP uptake by the addition of a second term -dN_1/dt, where N_1 is the number of internalised NPs. If we assume that the rate of uptake is proportional to the number of NPs present on the membrane, then $dN_1/dt=k_{m1}N_m$, where k_{m1} is the rate constant for internalisation. Solution of the full equation system then shows that the uptake rate, J, in the linear regime is given by

$$J(c_0) = N_{m,max}\, k_{m1}/(1 + (k_{m0} + k_{m1})/k_{0m}c_0) \qquad (2)$$

A two-parameter [$N_{m,max}k_{m1}$ and $(k_{m0}+k_{m1})/k_{0m}$] fit of Equation (2) to the uptake rates is shown in Figure 4b. The excellent agreement further confirms the importance of the adhesion process to NP uptake.

Conclusions

The presence of a protein corona reduces the free energy of the NP surface. For NPs with high energy of the bare surface the reduction is vast, and as a consequence the adhesion to the cell membrane of NP-protein complexes is strongly reduced compared to bare NPs. The lowered adhesion in turn affects uptake levels. Biomolecules in the corona may induce specific recognition by cell membrane receptors and cause regulated uptake, hence affecting internalisation rate. As the corona is different for NPs of different size and material, the extent to which this occurs depends on the detailed system. The lowered adhesion is, however, expected to be a common feature of NPs in a biological milieu, with particularly large manifestations for NPs with high energy of the bare surface.

On supported POPC lipid bilayers, bare NPs adsorb quickly and strongly; in fact, the adhesion is so strong that desorption could not be detected. The latter observation could not be corroborated for adsorption onto the cell membrane, where our data suggest desorption of NPs both in the absence and presence of proteins. This difference could be due to the different nature of the cell membrane, which is more complicated than a pure lipid bilayer containing also proteins, different types of lipids and other components.

The adhesion kinetics of NPs to the cell membrane exhibits signs of two processes: one fast adsorption that occurs within tens of minutes, followed by a slower process that has not concluded even after 3 h. Different possible interpretations for the presence of two processes can be given, though we are not able to differentiate between them further. We argue that NP uptake can be understood in terms of a two-step process: NPs, covered with protein corona or not, adhere to the cell membrane and interact with lipid and proteins of the membrane. The adhesion step is then followed by the activation of some energy-dependent uptake mechanism(s), which allows the NPs to be internalised by the cell.

The adhesion properties of NPs to the cell membrane are therefore key determinants of NP uptake rates and should be assessed together with the physico-chemical characterisation of the NP dispersion In this work we have used two methods to this end, both of which could be further extended to investigate different conditions. For instance, in the future the type of lipid could be varied or different lipid mixtures used for QCM-D studies, while the flow cytometry method could be applied to different cell types in order to investigate NP adhesion on different cell membranes. Regardless, the direct comparison of two methods allows a rather satisfactory characterisation of the NP adhesion properties, and how these change depending on the biological fluid and environment in which the NPs are found.

ASSOCIATED CONTENT

Supporting Information. Materials and methods, physico-chemical characterization of the nanoparticles used in the study and supporting experimental results. This material is available free of charge via the Internet at http://pubs.acs.org.

AUTHOR INFORMATION

Corresponding Authors

* christoffer.aberg@cbni.ucd.ie, kenneth.a.dawson@cbni.ucd.ie

Author Contributions

†These authors contributed equally.

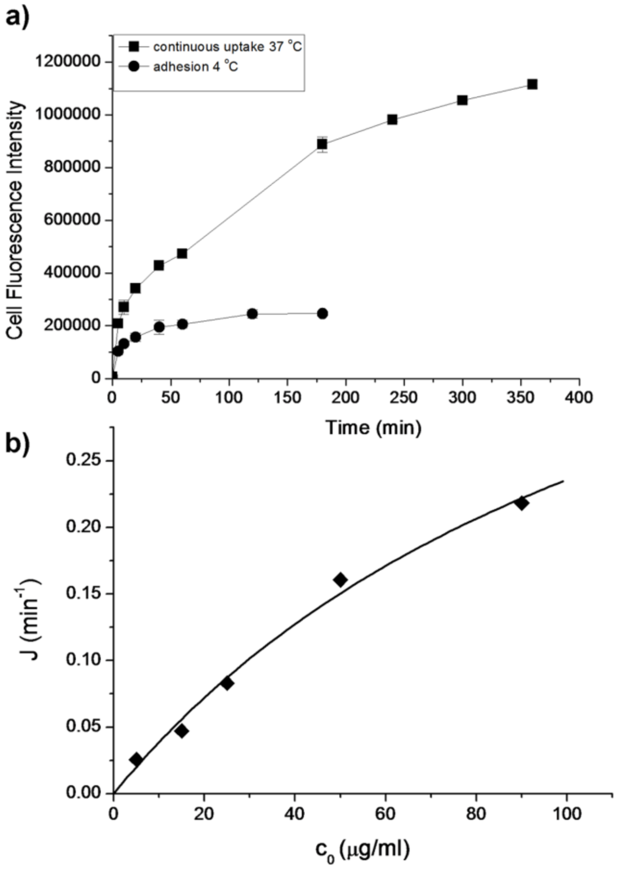

Figure 4. Relevance of adhesion to uptake levels. (a) Comparison of the uptake kinetics during continuous exposure and the adhesion kinetics of 40 nm PS-COOH NPs at 100 μg/ml in complete medium, as determined by flow cytometry. The uptake kinetics during continuous exposure (“continuous uptake 37 °C”) was assessed by exposing cells to NPs in complete medium at 37 °C for the indicated times (as in Figure 1); the adhesion kinetics (“adhesion 4 °C”) was assessed by exposing cells to NPs in complete medium at 4 °C for the indicated times, followed by further incubation for 3 h at 37 °C in NP-free complete medium (as in Figure 2). The mean cell fluorescence of 15,000 cells was determined for each replica. Data points and error bars represent the mean and standard deviation averaged over three replicas. (b) NP uptake rates during the linear regime as a function of extracellular NP concentration. Solid line shows a two-parameter fit to Equation 2 as described in the text. Data reproduced from previous work.[28]

Funding Sources

This work is based upon work supported by the Small Collaborative project NeuroNano funded by the European Commission 7th Framework Programme (NNP4-SL-2008-214547) (A.L.), the Irish Research Council for Science, Engineering and Technology (C.Å.), Science Foundation Ireland under Grant No. [09/RFP/MTR2425] (C.Å.), the European Union Seventh Framework Programme project NanoTransKinetics under grant agreement no. 266737 (C.Å.) and was conducted under the framework of the INSPIRE programme, funded by the Irish Government’s Programme for

Research in Third Level Institutions, Cycle 4, National Development Plan 2007-2013 (A.S.). Part of this work has been supported by Science Foundation Ireland (SFI) PI grant to M.W.R. M.J.S.M. is Ussher Lecturer in Pharmaceutical Drug Discovery Trinity College Dublin.

ACKNOWLEDGMENT

Use of the UCD Conway Flow Cytometry and Imaging Facilities is acknowledged. Dr. Eugene Mahon (CBNI, UCD) is kindly acknowledged for assistance with QCM-D measurements.

ABBREVIATIONS

NP, nanoparticle; QCM-D, Quartz Crystal Microbalance with Dissipation; PS-COOH, carboxylated polystyrene; sfMEM, serum free medium; cMEM, complete medium; HC, hard corona; POPC, 2-Oleoyl-1-palmitoyl-*sn*-glycero-3-phosphocholine.

REFERENCES

(1) Oberdörster, G.; Oberdörster, E.; Oberdörster, J. *Environ. Health Perspect.* **2005**, *113*, 823-839.

(2) Nel, A. E.; Mädler, L.; Velegol, D.; Xia, T.; Hoek, E. M. V.; Somasundaran, P.; Klaessig, F.; Castranova, V.; Thompson, M. *Nat. Mater.* **2009**, *8*, 543-557.

(3) Rivera Gil, P.; Oberdoïrster, G. n.; Elder, A.; Puntes, V. c.; Parak, W. J. *ACS Nano* **2010**, *4*, 5527-5531.

(4) Donaldson, K.; Stone, V.; Tran, C. L.; Kreyling, W.; Borm, P. J. A. *Occup. Environ. Med.* **2004**, *61*, 727-728.

(5) Shvedova, A. A.; Kagan, V. E.; Fadeel, B. *Annu. Rev. Pharmacol. Toxicol.* **2010**, *50*, 63-88.

(6) Khan, F. R.; Misra, S. K.; García-Alonso, J.; Smith, B. D.; Strekopytov, S.; Rainbow, P. S.; Luoma, S. N.; Valsami-Jones, E. *Environ. Sci. Technol.* **2012**, *46*, 7621-7628.

(7) Elder, A.; Vidyasagar, S.; DeLouise, L. *Wiley Interdisciplinary Rev. Nanomedicine Nanobiotechnol.* **2009**, *1*, 434-450.

(8) Ferrari, M. *Nat. Rev. Cancer* **2005**, *5*, 161-171.

(9) Farokhzad, O. C.; Langer, R. *ACS Nano* **2009**, *3*, 16-20.

(10) Rejman, J.; Oberle, V.; Zuhorn, I. S.; Hoekstra, D. *Biochem. J.* **2004**, *377*, 159-169.

(11) Chithrani, B. D.; Ghazani, A. A.; Chan, W. C. W. *Nano Lett.* **2006**, *6*, 662-668.

(12) Jiang, W.; Kim, B. Y. S.; Rutka, J. T.; Chan, W. C. W. *Nat. Nanotechnol.* **2008**, *3*, 145-150.

(13) dos Santos, T.; Varela, J.; Lynch, I.; Salvati, A.; Dawson, K. A. *Small* **2011**, *7*, 3341-3349.

(14) Dausend, J.; Musyanovych, A.; Dass, M.; Walther, P.; Schrezenmeier, H.; Landfester, K.; Mailänder, V. *Macromol. Biosci.* **2008**, *8*, 1135-1143.

(15) Cho, E. C.; Xie, J.; Wurm, P. A.; Xia, Y. *Nano Lett.* **2009**, *9*, 1080-1084.

(16) Brandenberger, C.; Mühlfeld, C.; Ali, Z.; Lenz, A.-G.; Schmid, O.; Parak, W. J.; Gehr, P.; Rothen-Rutishauser, B. *Small* **2010**, *6*, 1669-1678.

(17) Monopoli, M. P.; Åberg, C.; Salvati, A.; Dawson, K. A. *Nat. Nanotechnol.* **2012**, *7*, 779-786.

(18) Cedervall, T.; Lynch, I.; Lindman, S.; Berggård, T.; Thulin, E.; Nilsson, H.; Dawson, K. A.; Linse, S. *Proc. Natl. Acad. Sci. U. S. A.* **2007**, *104*, 2050-2055.

(19) Lundqvist, M.; Stigler, J.; Elia, G.; Lynch, I.; Cedervall, T.; Dawson, K. A. *Proc. Natl. Acad. Sci. U. S. A.* **2008**, *105*, 14265-14270.

(20) Aggarwal, P.; Hall, J. B.; McLeland, C. B.; Dobrovolskaia, M. A.; McNeil, S. E. *Adv. Drug Deliv. Rev.* **2009**, *61*, 428-437.

(21) Prapainop, K.; Witter, D. P.; Wentworth, J. P. *J. Am. Chem. Soc.* **2012**, *134*, 4100-4103.

(22) Kapralov, A. A.; Feng, W. H.; Amoscato, A. A.; Yanamala, N.; Balasubramanian, K.; Winnica, D. E.; Kisin, E. R.; Kotchey, G. P.; Gou, P.; Sparvero, L. J.; Ray, P.; Mallampalli, R. K.; Klein-Seetharaman, J.; Fadeel, B.; Star, A.; Shvedova, A. A.; Kagan, V. E. *ACS Nano* **2012**, *6*, 4147-4156.

(23) Walczyk, D.; Baldelli Bombelli, F.; Monopoli, M. P.; Lynch, I.; Dawson, K. A. *J. Am. Chem. Soc.* **2010**, *132*, 5761-5768.

(24) Monopoli, M. P.; Walczyk, D.; Campbell, A.; Elia, G.; Lynch, I.; Baldelli Bombelli, F.; Dawson, K. A. *J. Am. Chem. Soc.* **2011**, *133*, 2525-2534.

(25) Lynch, I.; Salvati, A.; Dawson, K. A. *Nat. Nanotechnol.* **2009**, *4*, 546-547.

(26) Lesniak, A.; Campbell, A.; Monopoli, M. P.; Lynch, I.; Salvati, A.; Dawson, K. A. *Biomaterials* **2010**, *31*, 9511-9518.

(27) Maiorano, G.; Sabella, S.; Sorce, B.; Brunetti, V.; Malvindi, M. A.; Cingolani, R.; Pompa, P. P. *ACS Nano* **2010**, *4*, 7481-7491.

(28) Salvati, A.; Åberg, C.; dos Santos, T.; Varela, J.; Pinto, P.; Lynch, I.; Dawson, K. A. *Nanomedicine Nanotechnol. Biol. Med.* **2011**, *7*, 818-826.

(29) Shapero, K.; Fenaroli, F.; Lynch, I.; Cottell, D. C.; Salvati, A.; Dawson, K. A. *Mol. BioSyst.* **2011**, *7*, 371-378.

(30) Wilhelm, C.; Gazeau, F.; Roger, J.; Pons, J. N.; Bacri, J. C. *Langmuir* **2002**, *18*, 8148-8155.

(31) Safi, M.; Courtois, J.; Seigneuret, M.; Conjeaud, H.; Berret, J. F. *Biomaterials* **2011**, *32*, 9353-9363.

(32) Doiron, A. L.; Clark, B.; Rinker, K. D. *Biotechnol. Bioeng.* **2011**, *108*, 2988-2998.

(33) Hou, W.-C.; Moghadam, B. Y.; Corredor, C.; Westerhoff, P.; Posner, J. D. *Environ. Sci. Technol.* **2012**, *46*, 1869-1876.

(34) Deng, Z. J.; Liang, M.; Monteiro, M.; Toth, I.; Minchin, R. F. *Nat. Nanotechnol.* **2011**, *6*, 39-44.

(35) Lesniak, A.; Fenaroli, F.; Monopoli, M. P.; Åberg, C.; Dawson, K. A.; Salvati, A. *ACS Nano* **2012**, *6*, 5845-5857.

(36) Zhu, Y.; Li, W.; Li, Q.; Li, Y.; Li, Y.; Zhang, X.; Huang, Q. *Carbon* **2009**, *47*, 1351-1358.

(37) Guarnieri, D.; Guaccio, A.; Fusco, S.; Netti, P. A. *J. Nanoparticle Res.* **2011**, *13*, 4295-4309.

(38) Bajaj, A.; Samanta, B.; Yan, H.; Jerry, D. J.; Rotello, V. M. *J. Mater. Chem.* **2009**, *19*, 6328-6331.

(39) Patel, P. C.; Giljohann, D. A.; Daniel, W. L.; Zheng, D.; Prigodich, A. E.; Mirkin, C. A. *Bioconj. Chem.* **2010**, *21*, 2250-2256.

(40) Kim, J. A.; Åberg, C.; Salvati, A.; Dawson, K. A. *Nat. Nanotechnol.* **2012**, *7*, 62-68.

(41) Tenuta, T.; Monopoli, M. P.; Kim, J. A.; Salvati, A.; Dawson, K. A.; Sandin, P.; Lynch, I. *PLoS ONE* **2011**, *6*.

(42) Tamm, L. K.; McConnell, H. M. *Biophys. J.* **1985**, *47*, 105-113.

(43) Richter, R. P.; Bérat, R.; Brisson, A. R. *Langmuir* **2006**, *22*, 3497-3505.

(44) Volinsky, R.; Cwiklik, L.; Jurkiewicz, P.; Hof, M.; Jungwirth, P.; Kinnunen, Paavo K. J. *Biophys. J.* **2011**, *101*, 1376-1384.

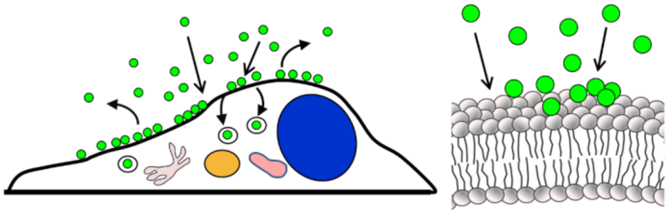Graphic entry for the Table of Contents (TOC)